

Limits and Convergence properties of the Sequentially Markovian Coalescent

Thibaut Sellinger^{1*}, Diala Abu Awad, Aurélien Tellier¹

¹ Professorship for Population Genetics,

Department of Life Science Systems,

Technical University of Munich

* Corresponding author, thibaut.sellinger@tum.de

1
2
3
4
5
6
7
8
9
10
11
12
13
14
15
16
17
18
19
20
21
22
23

Abstract

Many methods based on the Sequentially Markovian Coalescent (SMC) have been and are being developed. These methods make use of genome sequence data to uncover population demographic history. More recently, new methods even allow the simultaneous estimation of the demographic history and other biological variables, extending the original theoretical frameworks. Those methods can be applied to many different species, under different model assumptions, in hopes of unlocking the population/species evolutionary history. Although convergence proofs in particular cases have been given using simulated data, a clear outline of the performance limits of these methods is lacking. We here explore the limits of this methodology, as well as present a tool that can be used to help users quantify what information can be confidently retrieved from given datasets. In addition, we study the consequences for inference accuracy of the violation of hypotheses and assumptions of SMC approaches, such as the presence of transposable elements, variable recombination and mutation rates along the sequence and SNP call errors. We also provide a new interpretation of the SMC through the use of the estimated transition matrix and offer recommendations for the most efficient use of these methods under budget constraints, notably through the building of data sets that would be better adapted for the biological question at hand.

Keywords— Hidden Markov Model, Ancestral Recombination Graph, Popu-

lation Genetics

24 1 Introduction

25 Recovering the demographic history of a population has become a central theme in evo-
26 lutionary biology. The demographic history (the variation of effective population size
27 over time) is linked to environmental and demographic changes that existing and/or
28 extinct species have experienced (population expansion, colonization of new habitats,
29 past bottlenecks) [14, 42, 4]. Current statistical tools to estimate the demographic
30 history rely on genomic data [48] and these inferences are often linked to archaeolog-
31 ical or climatic data, providing new insights on their consequent genomic signatures
32 [67, 32, 43, 1, 12, 25, 24]. From these analyses, evidence for migration events have been
33 uncovered [25, 5], as have genomic consequences of human activities on other species
34 [9]. Linking demographic history to climate and environmental data greatly supports
35 the field of conservation genetics [10, 17, 39]. Such analyses can help ecologist in de-
36 tecting effective population size decrease [65], and thus serve as a guide in maintaining
37 or avoiding the erosion of genetic diversity in endangered populations, and potentially
38 predicting the consequences of climate change on genetic diversity [26]. In addition,
39 studying the demographic histories of different species in relation to one another can
40 unveil latent biological or environmental evolutionary forces [16], unveiling links and
41 changes within entire ecosystems. With the increased accuracy of current methods,
42 the availability of very large and diverse data sets and the development of new theoret-
43 ical frameworks, the demographic history has become an information that is essential
44 in the field of evolution [45, 6]. However, unbiased estimations and interpretations of
45 the demographic history remain challenging [3, 8].

46 The most sophisticated methods to infer demographic history make use of
47 whole genome polymorphism data. Among the state of the art methods, some are

48 based on the theory of the Sequentially Markovian Coalescent (SMC) developed by
49 [34] after the work of [66], corrected by [30] and first applied to whole genome se-
50 quences by [25], who introduced the now well known Pairewise Sequentially Marko-
51 vian Coalescent (PSMC) method. PSMC allows demographic inference of the whole
52 population with unprecedented accuracy, while requiring only one sequenced diploid
53 individual. This method uses the distribution of SNPs along the genome between
54 the two sequences to account and infer recombination and demographic history of a
55 given population, assuming neutrality and a panmictic population. Although PSMC
56 was a breakthrough in demographic inference, it has limited power in inferring more
57 recent events. In order to address this issue, PSMC has been extended to account
58 for multiple sequences (*i.e.* more than two) into the method known as the Multiple
59 Sequentially Markovian Coalescent (MSMC) [47]. By using more sequences, MSMC
60 better infers recent events and also provides the possibility of inferring population
61 splits using the cross-coalescent rate. MSMC, unlike PSMC, is not based on SMC
62 theory [34] but on SMC' theory [30], therefore MSMC applied to only 2 sequences has
63 been defined as PSMC'. Methods developed after MSMC followed suit, with MSMC2
64 [29] extending PSMC by incorporating pairwise analysis, increasing efficiency and the
65 number of sequences that can be inputted (up to a hundred), resulting in more accu-
66 rate results. SMC++ [60] brings the SMC theory to another level by allowing the use
67 of hundreds of unphased sequences (MSMC requires phased input data) and breaking
68 the piece-wise constant population size hypothesis, while accounting for the sample
69 frequency spectrum (SFS). Because SMC++ incorporates the SFS in the estimation
70 of demographic history, it increases accuracy in recent time [60]. SMC++ is currently
71 the state of the art SMC based method for big data sets (>20 sequences), but seems
72 to be outperformed by PSMC when using smaller data sets [44]. In a similar vein,

73 the Ascertained Sequentially Markovian Coalescent (ASMC) [41] extends the SMC
74 theory to estimate coalescence times at the locus scale from ascertained SNP array
75 data, something that was made possible by the theory developed by [18].

76 More recently, a second generation of SMC based methods have been developed.
77 New features have been added to the initial SMC theory, extending their application
78 beyond simply inferring past demography [1, 50, 63]. The development of C-PSMC
79 [16] allows the interpretation of estimated demographic history in the light of coevo-
80 lution, making the first link between demographic history estimated by PSMC and
81 evolutionary forces (although biological interpretation remains limited). iSMC [1] ex-
82 tends the PSMC theory to account and infer the variation of recombination rate along
83 sequences, unlocking recombination map estimations. An impressive advancement is
84 the development of IS-MSMC, which solves to some extent the population structure
85 problem, allowing accurate and simultaneous inference of the demographic history and
86 population admixture [63]. eSMC [50] incorporates common biological traits (such as
87 self-fertilization and dormancy) and demonstrated the strong effect life history traits
88 can have on demographic history estimations. Results which may not be explained
89 under the initial SMC hypotheses can now be explained by the potential presence of
90 measurable phenomena not present in the original PSMC.

91 New methods have been developed since PSMC, that have been either strongly
92 inspired by the SMC [51, 59] or that are completely dissociated from it [55, 2, 46, 20,
93 28, 19, 54, 62]. Though there are alternative approaches, methods based on the SMC
94 are still considered state of the art, and remain widely used [31, 3, 56], notably in
95 human evolution studies [56, 44]. However, each described method has its specificity,
96 designed to solve a specific problem using specific data based on different hypothesis.

97 Although all these methods allow a new and different interpretation of genomic data,
98 none of these methods guarantees unbiased inference, and their limitations have rather
99 underlined how crucial and challenging demographic inference is, highlighting the com-
100 plementarity and usefulness to use several inference methods on a given dataset.

101 SMC based methods display very good fits when using simulated data, espe-
102 cially when using simple single population model based on typical human data param-
103 eters [60, 47, 50, 63]. However, the SMC makes a large number of hypotheses [25, 47]
104 that are often violated in data obtained from natural populations. When inputting
105 data from natural populations, extracting information or correctly interpreting the
106 results can become troublesome [8, 61, 3] and several studies address the consequences
107 of hypothesis violation [15, 8, 46, 33, 49]. They bring to light how strongly population
108 structure or introgression influence demographic history estimation if not correctly ac-
109 counted for [15, 8]. Furthermore, most SMC based methods require phased data (such
110 as MSMC and IS-MSMC), and phasing errors can lead to strong overestimation of
111 population size in recent time [60]. The effect of coverage during sequencing has also
112 been tested in [36], showing the importance of high coverage in order to obtain trust-
113 worthy results, and yet, SMC methods seem robust to genome quality [44]. Selection,
114 if not accounted for, can result in a bottleneck signature [49], and there is currently no
115 solution to this issue within the SMC theory, though it could be addressed using differ-
116 ent theoretical frameworks that are being developed [52, 37]. More problematic, is the
117 ratio of effective recombination over effective mutation rates $\frac{\rho}{\theta}$. If the ratio is greater
118 than one, biases in estimations are to be expected [60, 1, 50]. It is also important to
119 keep in mind that there can be deviations between $\frac{\rho}{\theta}$ and the ratio of recombination
120 rate over mutation rates measured experimentally ($\frac{r}{\mu}$), as the former can be greatly

121 influenced by life-history and this can lead to issues when interpreting results (*e.g.*
122 [50]). It is thus necessary to keep in mind that the accuracy of SMC based methods
123 depends on which of the many underlying hypothesis are prone to being violated by
124 the data sets being used.

125 In an attempt to complement previous works, we here offer to study the limits
126 and the convergences properties of methods based on the Sequentially Markovian Coa-
127 luescence. We first define the limits of SMC based methods (*i.e.* how well they perform
128 theoretically), which we will call the theoretical convergence, using a similar approach
129 to [13, 40, 19] by giving the simulated genealogy as input. We test several scenarios
130 to check whether there are instances, where even without violating the underlying hy-
131 potheses of the methodology, the demographic scenarios cannot be retrieved because
132 of theoretical limits (and not issues linked with data). We then compare simulation
133 results obtained with the genealogy given as input to results obtained from sequences
134 simulated under the same genealogy, so as to study the convergence properties linked
135 to data sets in the absence of hypothesis violation. We also study the effect of the
136 optimization function (or composite likelihood) and the time window of the analysis
137 on the estimations of different variables. Lastly, we test the effect of commonly vi-
138 olated hypotheses, such as the effect of the variation of recombination and mutation
139 rates along the sequence and between scaffolds, errors in SNP calls and the presence
140 of transposable elements and link abnormal results to specific hypothesis violations.
141 Through this work, our aim is to provide guidelines concerning the interpretation of
142 results when applying this methodology on data sets that may violate the underlying
143 hypotheses of the SMC framework.

144 2 Materials and Methods

145 In this study we use four different SMC-based methods: MSMC, MSMC2, SMC++
146 and eSMC. All methods are Hidden Markov Models and use whole genome sequence
147 polymorphism data. The hidden states of these methods are the coalescence times
148 (or genealogies) of the sample. In order to have a finite number of hidden state (and
149 parameters), the hidden states are grouped into x discretized bins (x being the number
150 of hidden states). The reasons for our model choices are as follows. MSMC, unlike
151 any other method, focuses on the first coalescent event of a sample of size n , and thus
152 exhibits different convergence properties [47]. MSMC2 computes coalescent times of all
153 pairwise analysis from a sample of size n , and can deal with a large range of data sets
154 [55]. SMC++ [60] is the most advanced and efficient SMC method which can make use
155 of hundreds sequences, enabling the use of the SFS along the sequence. Lastly, eSMC
156 [50] is a re-implementation of PSMC' (similar to MSMC2), which will contribute to
157 highlighting the importance of algorithmic translations as it is very flexible in its use
158 and outputs intermediate results necessary for this study.

159 2.1 SMC methods

160 2.1.1 PSMC', MSMC2 and eSMC

161 PSMC' and methods that stem from it (such as MSMC2 [29] and eSMC [50]) focus on
162 the coalescence events between only two individuals (or sequences in practice), and,
163 as a result, does not require phased data. The algorithm goes along the sequence
164 and estimates the coalescence time at each position. In order to do this, it checks
165 whether the two sequences are similar or different at each position. If the two sequences
166 are different, this indicates a mutation took place, and, as mutations are considered

167 uncommon, that the common ancestor is far in the past. An absence of mutation
168 (the two sequences are identical) suggests a recent common ancestor. In the event
169 of recombination, there is a break in the current genealogy and the coalescence time
170 consequently takes a new value. A detailed description of the algorithm can be found
171 in [47, 63, 50].

172 **2.1.2 MSMC**

173 MSMC is mathematically and conceptually very similar to the PSMC' method. Un-
174 like other SMC methods, it simultaneously analyses multiple sequences and because
175 of this, MSMC requires the data to be phased. In combination with a second HMM,
176 to estimate the external branch length of the genealogy, it can follow the distribution
177 of the first coalescence event in the sample along sequences. However, MSMC can-
178 not analyze more than 10 sequences simultaneously (due to computational load). A
179 detailed description of MSMC can be found in [47].

180 **2.1.3 SMC++**

181 SMC++ is slightly more complex than MSMC or PSMC, though it is conceptually
182 very similar to PSMC', mathematically it is quite different. SMC++ has a different
183 emission matrix compared to previous methods because it calculates the sample fre-
184 quency spectrum of sample size $n + 2$, conditioned on the coalescence time of two
185 "distinguished" haploids and n "undistinguished" haploids. In addition SMC++ of-
186 fers features like a cubic spline to estimate demographic history (*i.e.* not a piece-wise
187 constant population size). The SMC++ algorithm is fully described in [60].

188 **2.1.4 Theoretical convergence**

189 Using sequence simulators such as msprime [21] or scrm [57], one can simulate the
190 Ancestral Recombination Graph (ARG) of a sample. Usually the ARG is given through
191 a sequence of genealogies (*e.g.* a sequence of trees in Newick format). From this ARG,
192 one can find what state of the HMM the sample is in at each position. Hence, one
193 can build the series of states along the genomes, and build the transition matrix.
194 The transition matrix, is a square matrix (of dimension x defined as the number of
195 hidden states) counting the number of transitions from one of the x state to another
196 (it also counts the number of transitions from one state to the same state). Using the
197 transition matrix built directly from the exact ARG, one can estimate parameters using
198 PSMC' or MSMC as if they could perfectly infer the hidden states. Hence estimations
199 using the exact transition matrix represents the upper bound of performance for those
200 methods. We choose to call this upper bound the theoretical convergence (since it
201 can never be reached in practice). For this study's purpose, a second version of the R
202 package eSMC [50] was developed. This package enables the building of the transition
203 matrix (for PSMC' or MSMC), and can then use it to infer the demographic history.
204 The package is mathematically identical to the previous version, but includes extra
205 functions, features and new outputs necessary for this study. The package and its
206 description can be found at <https://github.com/TPPSellinger/eSMC2>.

207 **2.1.5 Baum-Welch algorithm**

208 SMC based method can use different optimization functions to infer the demographic
209 parameters (*i.e.* likelihood or composite likelihood). The four studied methods use
210 the Baum-Welch algorithm to maximize the likelihood. MSMC2 and SMC++ imple-
211 ment the original Baum-Welch algorithm (which we call the complete Baum-Welch

212 algorithm), whereas PSMC' and MSMC compute the expected composite likelihood
 213 $Q(\theta|\theta^t)$ based only on the transition matrix (which we call the incomplete Baum-
 214 Welch algorithm). The use of the complete Baum-Welch algorithm or the incomplete
 215 one can be specified in the eSMC package. The composite likelihood for SMC++ and
 216 MSMC2 is given by equations 1 and the composite likelihood for PSMC' and MSMC
 217 by equation 2:

$$Q(\theta|\theta^t) = \nu_{\theta^t} \log(P(X_1|\theta)) + \sum_{X,Y} E(X, Z|\theta^t) \log(P(X|Z, \theta)) + \sum_{X,Y} E(Y, X|\theta^t) \log(P(Y|X, \theta)) \quad (1)$$

218 and :

$$Q(\theta|\theta^t) = \sum_{X,Y} E(X, Z|\theta^t) \log(P(X|Z, \theta)), \quad (2)$$

219 with:

- 220 • ν_{θ} : The equilibrium probability conditional to the set of parameters θ
- 221 • $P(X_1|\theta)$: The probability of the first hidden state conditional to the set of
 222 parameters θ
- 223 • $E(X, Z|\theta^t)$: The expected number of transitions of X from Z conditional to the
 224 observation and set of parameters θ^t
- 225 • $P(X|Z, \theta)$: The transition Probability from state Z to state X, conditional to
 226 the set of parameters θ
- 227 • $E(Y, X|\theta^t)$ The expected number of observations of type Y that occurred during
 228 state X conditional to observation and set of parameters θ^t
- 229 • $P(Y|X, \theta)$: The emission probability conditional to the set of parameters θ

230 **2.1.6 Time window**

231 Each tested SMC based method has its own specific time window in which estimations
232 are made. As for example, the original PSMC has a time window wider than PSMC'.
233 To measure the effect of the time window we analyze the same data with 4 different
234 time windows. The first time window is the one of PSMC' defined in [47]. The second
235 time window is the one of MSMC2 [63] (similar to the one of the original PSMC [25]),
236 which we call "big" since it goes further in the past and in more recent time than the
237 one of PSMC'. We then define a time window equivalent to the first one (*i.e.* PSMC')
238 shifted by a factor 5 in the past (*first time window multiplied by 5*). The last window
239 is a time window equivalent to the first one shifted by a factor 5 in recent time (*first*
240 *time window divided by 5*).

241 **2.2 Simulated Sequence data**

242 Throughout this paper we simulate different demographic scenarios using either the
243 coalescence simulation program scrm [57] or msprime [21]. We use scrm for the the-
244 oretical convergence as it can output the genealogies in a Newick format (which we
245 use as input). We use msprime to simulate data for SMC++ since msprime is more
246 efficient than scrm for big sample sizes [21] and can directly output .vcf files (which is
247 the input format of SMC++).

248 **2.2.1 Absence of hypothesis violation**

249 We simulate four demographic scenarios: saw-tooth (successions of population size
250 expansion and decrease), bottleneck, expansion and decrease. Each scenario is tested
251 under four amplitude parameters (*i.e.* by how many fold the population size varies:
252 2, 5, 10, 50). For each analysis we simulate four different sequence lengths (10^7 ,

253 10^8 , 10^9 and 10^{10} bp) and choose the per site mutation and recombination rates
254 recommended for human on the guide to MSMC, respectively 1.25×10^{-8} and 1×10^{-8}
255 (<https://github.com/stschiff/msmc/blob/master/guide.md>), all the command lines to
256 simulate data can be found in S1 of the Appendix. For each simulated data set, as
257 previously mentioned, four different algorithms are used to estimate the demographic
258 history and the recombination rate: eSMC, MSMC and MSMC2 and SMC++ (the
259 command lines to launch the analyses can be found in S2 of the Appendix).

260 **2.2.2 Presence of hypothesis violation**

261 **SNP calling:** In practice, SNP calling from next generation sequencing can yield
262 different numbers and frequencies of SNPs depending on the chosen parameters for
263 the different steps of analysis (read trimming, quality check, read mapping, and SNP
264 calling) as well as the quality of the reference genome, data coverage and depth of
265 sequencing, species ploidy and many more. Therefore, based on raw sequence data,
266 stringent filters can exclude SNPs (false negatives) or include serious SNPs (false
267 positives). When dealing with complex genomes or ancient DNA [53, 7], SNPs can be
268 simultaneously missed and added. We thus simulate sequences under a "saw-tooth"
269 scenario and then a certain percentage (5,10 and 25 %) of SNPs is randomly added
270 to and/or deleted from the simulated sequences. We then analyse the variation and
271 bias in SNP call on the accuracy of demographic parameter estimations.

272 **Changes in mutation and recombination rates along the sequence:**

273 Because the recombination rate and the mutation rate can change along the sequence[1],
274 and chromosomes are not always fully assembled in the reference genome (which con-
275 sists of possibly many scaffolds), we simulate short sequences where the recombination

276 and/or mutation rate randomly changes between the different scaffolds around an
277 average value of 1.25×10^{-8} per generation per base pair (between 2.5×10^{-9} and
278 6.25×10^{-8}). We chose to simulate 20 scaffolds of size 2 Mb, as this can represent
279 the best available assembly for non-model organisms [27, 58]. We then analyze the
280 simulated sequences to study the effect of assuming scaffolds sharing same mutation
281 and recombination rates. In addition, we simulate sequences of 40 Mb (assuming
282 genome fully assembled) where the recombination rate along the sequence randomly
283 changes every 2 Mbp (up to five-fold) around an average value of 1.25×10^{-8} (the
284 mutation rate being fixed at 1.25×10^{-8} per generation per bp) to study the effect of
285 the assumption of a constant recombination rate along the sequence.

286 **Transposable elements (TEs):** Genomes can contain transposable elements
287 which dynamics violate the classic infinite site mutational model for SNPs, and thus
288 potentially affecting the estimation of different parameters. Although methods have
289 been developed to detect [38] and simulate them [23], understanding how their pres-
290 ence/absence affect the demographic estimations remains unclear. TEs are usually
291 masked in the reference genome and thus not taken into account in the mapped indi-
292 viduals due to the redundancy of read mapping for TEs. To best capture and mimic
293 the effect of TEs in data, we altered simulated sequence data in two different ways.
294 Due to the repetitive nature of TEs, it can be difficult using short reads to correctly
295 detect and assemble them, as well as to assess their presence/absence polymorphism
296 across individuals of a population [11]. One way to simulate the effect of TEs is to as-
297 sume they exhibit presence/absence polymorphism thus creating gaps in the sequence.
298 For each individual, we therefore randomly remove small pieces from the original sim-
299 ulated sequence, thus shortening and fragmenting the whole sequence to be analyzed.

300 The second way, would be to assume that TEs are masked, a process which we simulate
301 by randomly selecting small pieces of sequence from the original simulated sequence,
302 and removing all the SNPs found in those regions (*i.e.* removing mutations from TEs
303 which could be used for inference but actually are judged to be non-reliable). In the
304 latter, the removed SNPs are structured in many small regions along the genome, and
305 not randomly missing throughout it. We also test the consequences of simultaneously
306 having both removed and masked TEs in the data set.

307 **3 Results**

308 We first study the theoretical accuracy and convergence properties of PSMC' and
309 MSMC methodologies using the sequence exact genealogies. We then analyze the
310 simulated sequences themselves and compare results between different SMC based
311 methods. Lastly, we analyze simulated sequences for which hypotheses made in the
312 SMC framework are violated, so as to study their impact on the accuracy of inference.

313 **3.1 Theoretical convergence**

314 Results of the theoretical convergence of PSMC' under the saw-tooth demographic
315 history are displayed in Figure 1. Increasing the sequence length increases accuracy
316 and reduces variability, leading to a perfect fit (see Figures 1a-c). However, when the
317 amplitude of population size variation is too great (here for 50 fold), the demographic
318 history cannot be retrieved, even when using very large data sets (see Figure 1d).
319 Similar results are obtained for the three other demographic scenarios (bottleneck,
320 expansion and decrease, respectively displayed in Supplementary Figures 1, 2 and 3).
321 The bottleneck scenario seems especially difficult to infer, requiring large amounts of

322 data, and the stronger the bottleneck, the harder it is to detect it, even with sequence
323 lengths equivalent to 10^{10} bp. In Supplementary Figure 4, we show that even when
324 changing the number of hidden states (*i.e.* number of inferred parameters), some
325 scenarios with very strong variation of population size are badly inferred when using
326 PSMC' based methods.

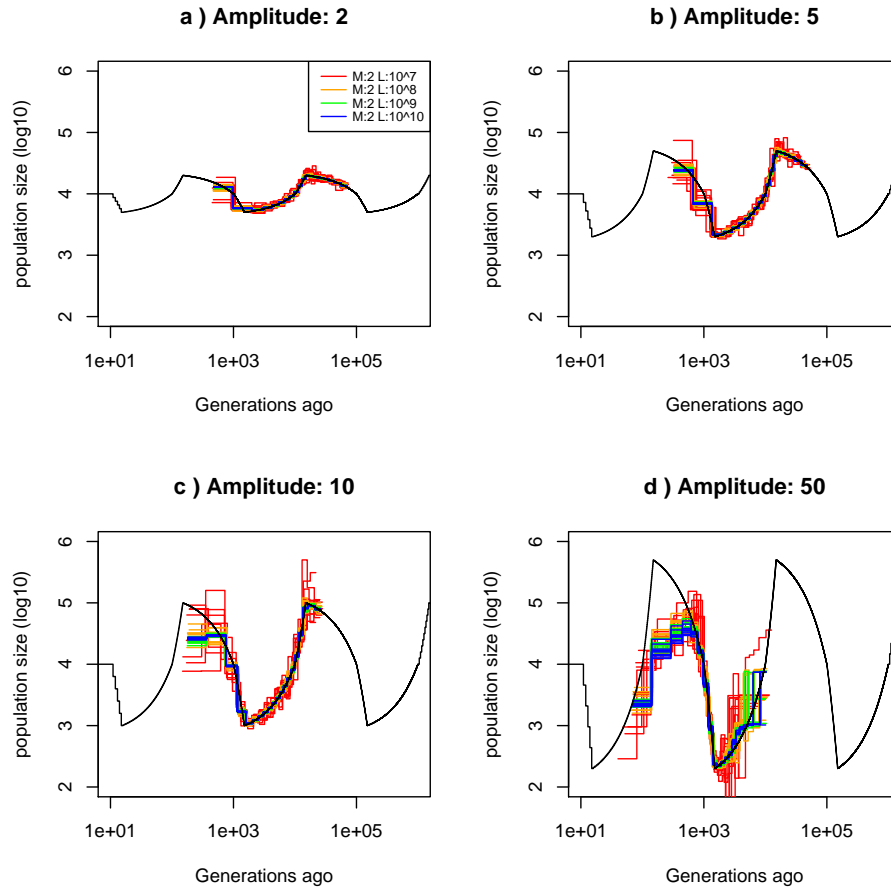


Fig. 1. Theoretical convergence of PSMC' Estimated demographic history using simulated genealogy over sequences of 10,100,1000,10000 Mb (respectively in red,orange, green and blue) under a saw-tooth scenario (black) with 10 replicates for different amplitudes of size change: a) 2-fold, b) 5-fold, c) 10-fold, and d) 50-fold. The recombination rate is set to 1×10^{-8} per generation per bp and the mutation rate to 1.25×10^{-8} per generation per bp.

327

In Supplementary Figures 5, 6, 7 and 8, we show the theoretical convergence

328 of MSMC with four genome sequences and generally find that these analyses present
329 a higher variance than PSMC'. However, MSMC shows better fits in recent times
330 than PSMC' and is better able to retrieve population size variation than PSMC' (see
331 Supplementary Figure 5d). Scenarios with strong variation of population size (*i.e.* with
332 large amplitudes) still pose a problem (see Supplementary Figure 9), and no matter
333 the number of estimated parameters, such scenarios cannot be correctly inferred using
334 MSMC.

335 To better understand these results, we examine the coefficient of variation
336 obtained from the distribution of the transition matrix. We can see that increasing the
337 sequence length reduces the coefficient of variation (the ratio of the standard deviation
338 to the mean, hence indicating convergence when equal to 0, see Supplementary Figure
339 10), but that for scenarios with a large amplitude of population size variation, some
340 hidden state transitions are not at all observed because of a lack of coalescence events
341 occurring in those specific time windows. This results in matrices displaying higher
342 coefficients of variation or no specific transition observed leading to a matrix that
343 is partially empty (Figure 2). This explains the increase of variability of the inferred
344 scenarios, as well as the incapacity of SMC methods to correctly infer the demographic
345 history with strong population size variation in specific time window.

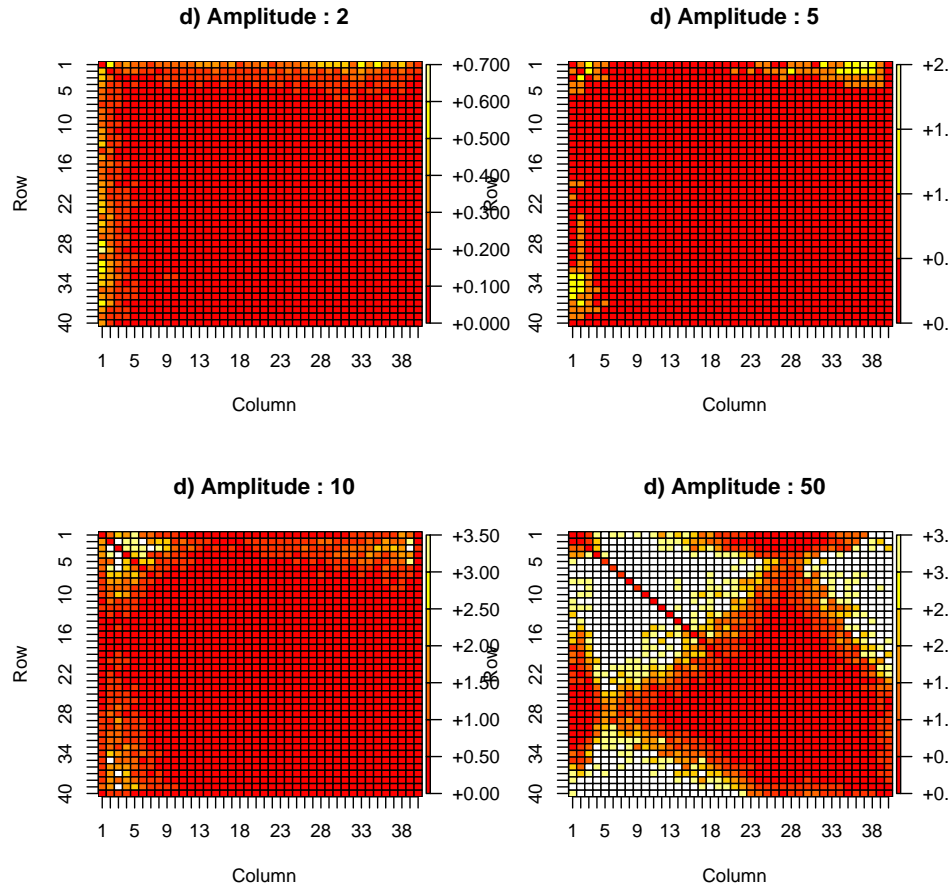


Fig. 2. Estimated transition matrix in sharp saw-tooth scenario Estimated coefficient of variation of the transition matrix using simulated genealogy over sequences of 10000 Mb under a saw-tooth scenario of amplitude 2, 5, 10 and 50 (respectively in a, b, c and d) each with 10 replicates with recombination and mutation rates are as in Figure 1. White squares indicate absence of observed transition (*i.e.* *no data*).

346 **3.2 Simulated sequence results**

347 **3.2.1 Scenario effect**

348 In the previous section, we explored the theoretical performance limitations of PSMC'
349 and MSMC using trees in Newick format as input. In this section, we evaluate how
350 these methods perform when inputting sequence data simulated under the same sce-
351 narios and parameters as above. Results for the saw-tooth scenario are displayed in
352 Figure 3, where the different models display a good fit, but are not as good as expected
353 from the theoretical convergence given the same amount of data (Figure 1 (orange line)
354 vs Figure 3 (red line)). As predicted by Figures 1 and 2, the case with the greatest
355 amplitude of population size variation (Figure 1d) is the least well fitted. All estima-
356 tions display low variance and a relatively good fit in the bottleneck and expansion
357 scenarios for small population size variation (see Supplementary Figures 11a and 12a
358). However, the strengths of expansions and bottlenecks are not fully retrieved in
359 scenarios with population size variation equal to or higher than tenfold the current
360 population size (Supplementary Figures 11c-d, and 12c-d). To study the origin of dif-
361 ferences between simulation results and theoretical results, we measure the difference
362 between the transition matrix estimated by eSMC and the one built from the actual
363 genealogy. Results show that hidden states are harder to find in scenarios which strong
364 population size variation, explaining the high variance (see Supplementary Figure 13).

365

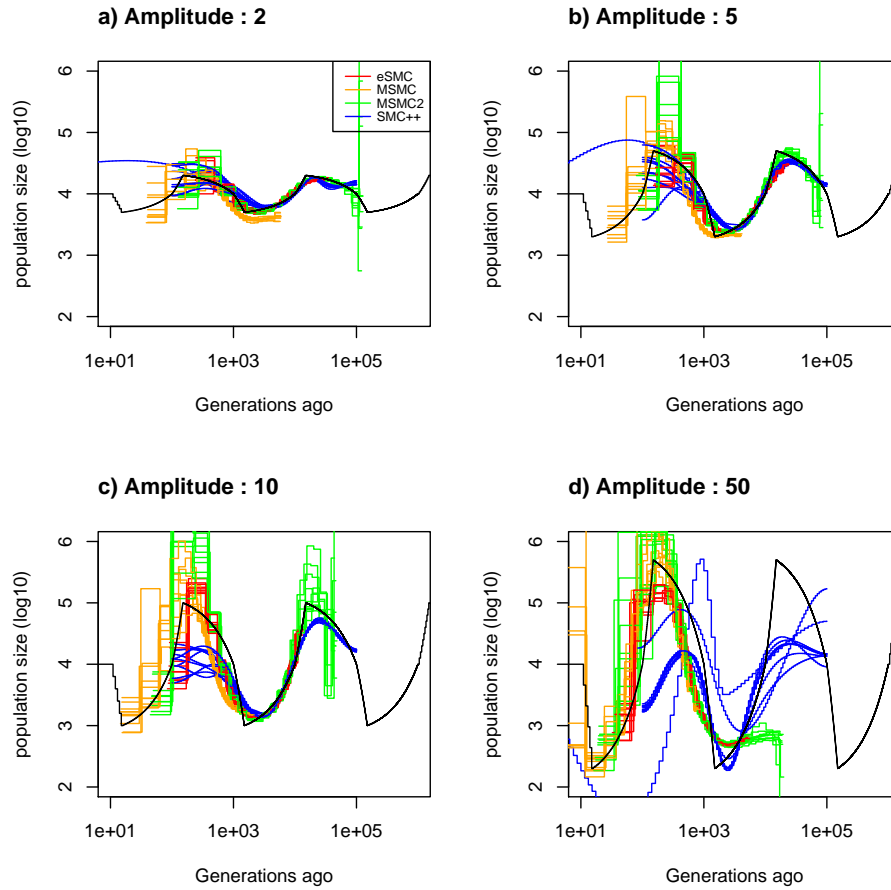


Fig. 3. Estimated demography using simulated sequences as input. Estimated demographic history (black) under a saw-tooth scenario with 10 replicates using simulated sequences for different amplitude of population size change: a) 2, b) 5, c) 10 and d) 50. Two sequences of 100 Mb for eSMC and MSMC2 (respectively in red and green). Four sequences of 100 Mb for MSMC (orange) and 20 sequences of 10 Mb for SMC++ (blue). Recombination and mutation rates are as in previous figures.

367 (Supplementary Figure 14). In addition, shifting the window towards more recent time
 368 leads to poor demographic estimation, but shifting it further in the past does not seem
 369 to bias the demographic estimation (there are however consequences on estimations of
 370 the recombination rates, see Table 1 for more details). Concerning the optimization
 371 function, we find that the complete Baum-Welch algorithm gives similar results to the
 372 incomplete one.

Optimization function	Scenario	real $\frac{\rho}{\theta}$	normal window $\frac{\rho}{\theta}^*$	Big Window $\frac{\rho}{\theta}^*$	Old window $\frac{\rho}{\theta}^*$	Recent window $\frac{\rho}{\theta}^*$
Incomplete Baum-Welch	Saw-tooth	0.8	0.79 (0.036)	0.72 (0.039)	0.72 (0.042)	0.94 (0.005)
Complete Baum-Welch	Saw-tooth	0.8	.79 (0.044)	0.72 (0.039)	0.72 (0.042)	1.56 (0.087)
Incomplete Baum-Welch	Constant	0.8	0.86 (0.019)	0.85 (0.020)	0.84 (0.019)	0.98 (0.002)
Complete Baum-Welch	Constant	0.8	0.86 (0.019)	0.85 (0.020)	0.84 (0.019)	1.06 (0.02)

Table 1: Average estimated values for the recombination over mutation ratio $\frac{\rho}{\theta}$ over ten repetitions for different size of the time window. The coefficient of variation is indicated in brackets. four sequences of 50 Mb simulated with a recombination rate set to 1×10^{-8} per generation per bp and a mutation rate to 1.25×10^{-8} per generation per bp.

373 3.2.2 Effect of the ratio of the recombination over the mutation rate

374 The ratio of the effective recombination over effective mutation rates ($\frac{\rho}{\theta}$) can influence
 375 the ability of SMC-based methods to retrieve the coalescence time between two points
 376 along the genome [60]. Intuitively, if recombination occurs at a higher rate compared
 377 to mutation, then it renders it more difficult to detect any recombination events that
 378 may have taken place before the introduction of a new mutation, and thus bias the
 379 estimation of the coalescence time [50, 60]. Under the bottleneck scenario, we find
 380 that the lower $\frac{\rho}{\theta}$, the better the fit of the inferred demography, but also the higher

381 the variance of the inferences (see Figure 4). SMC++ seems especially sensitive to
382 $\frac{\rho}{\theta}$. When calculating the difference between the transition matrix estimated by eSMC
383 (*i.e.* PSMC') and the one built from the actual genealogy (using Newick trees), we find
384 that, unsurprisingly, changes in hidden states are harder to detect when $\frac{\rho}{\theta}$ increases,
385 leading to an overestimation of hidden states on the diagonal (see Supplementary
386 Figures 15,16 and 17).

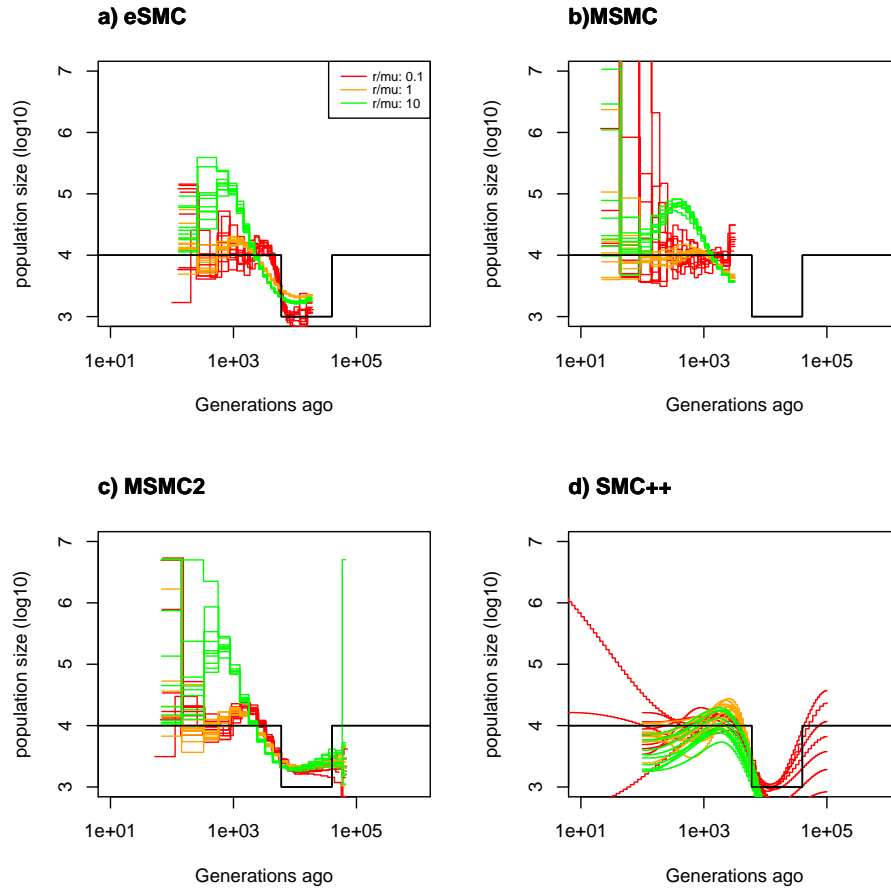


Fig. 4. Effect of $\frac{r}{\theta}$ on inference of demographic history. Estimated demographic history under a bottleneck scenario with 10 replicates using simulated sequences. Two sequences of 100 Mb for eSMC and MSMC2 (respectively in a and b). We use four sequences of 100 Mb for MSMC (c) and twenty sequences of 100 Mb for SMC++ (d). The mutation rate is set to 1.25×10^{-8} per generation per bp and the recombination rates are 1.25×10^{-9} , 1.25×10^{-8} and 1.25×10^{-7} per generation per bp, giving $\frac{r}{\theta} = 0.1, 1$ and 2 and the inferred demographies are in red, orange and green respectively. The demographic history is simulated under a bottleneck scenario of amplitude 10 and is represented in black.

387 It is, in some instances, possible to compensate for a $\frac{\rho}{\theta}$ ratio that is not ideal,
 388 by increasing the number of iterations. Indeed, for eSMC, the demographic history is
 389 better inferred (see Supplementary Figure 18), although the correct recombination rate
 390 cannot be retrieved (Table 2). MSMC is able to retrieve the correct recombination
 391 rate despite a high $\frac{\rho}{\theta}$, but poorly estimates the demographic history. The results
 392 obtained using MSMC2 and SMC++ are not improved when increasing the number
 393 of iterations (see Supplementary Figure 18 and Table 2).

method	real $\frac{\rho}{\theta}$	set 1 , $\frac{\rho^*}{\theta}$	set 2 , $\frac{\rho^*}{\theta}$	set 3 , $\frac{\rho^*}{\theta}$	set 4 , $\frac{\rho^*}{\theta}$	set 5 , $\frac{\rho^*}{\theta}$
eSMC	10	1.35 (0.026)	1.76 (0.047)	1.29 (0.027)	1.74 (0.048)	1.80 (0.041)
MSMC	10	2.70 (0.011)	6.58 (0.031)	2.68 (0.011)	6.57 (0.032)	6.62 (0.030)
MSMC2	10	1.27 (0.055)	1.65 (0.13)	1.26 (0.060)	1.75 (0.060)	1.60 (0.29)
SMC++	10	0.69 (0.34)	0.60 (0.45)	0.54 (0.15)	0.12 (0.66)	0.77 (.40)

Table 2: Average estimated values for the recombination over mutation ratio $\frac{\rho}{\theta}$ over ten repetitions. The coefficient of variation is indicated in brackets. For eSMC,MSMC and MSMC2 we have : set 1 : 20 hidden states; set 2 : 200 iterations ; set3 : 60 hidden states ; set 4 : 60 hidden states and 200 iterations and set 5 : 20 hidden states and 200 iterations. For SMC++; set 1 : 16 knots ; set 2 : 200 iterations ; set 3 : 4 knots in green; set 4: regularization penalty set to 3 and set 5 : regularization-penalty set to 12 .

394 3.3 Simulation results under hypothesis violation

395 3.3.1 Imperfect SNP calling

396 We analyze simulated sequences that have been modified by removing and/or adding
 397 SNPs using the different SMC methods. We find that, when using MSMC2, eSMC and
 398 MSMC, having more than 10 % of spurious SNPs can lead to a strong over-estimation

399 of population size in recent time but that missing SNPs have no effects on inferences
400 in the far past and only mild effects on inferences of recent time (see Figure 5 for
401 MSMC2 and Supplementary Figures 19 and 20 for eSMC and MSMC respectively).

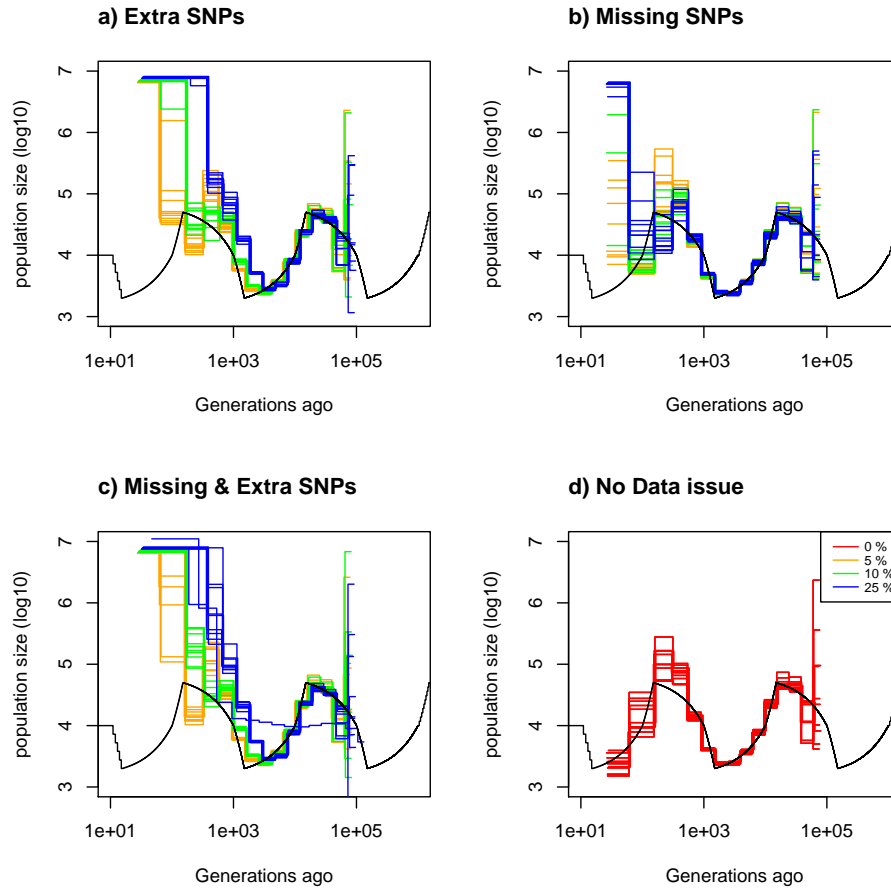


Fig. 5. Consequences of SNP calling errors. Estimated demographic history using MSMC2 under a saw-tooth scenario with 10 replicates using four simulated sequences of 100 Mb. Recombination and mutation rates are as in Figure 1 and the simulated demographic history is represented in black. a) Demographic history simulated with 5% (orange), 10% (green) and 25% (blue) missing SNPs. b) Demographic history simulated with 5% (orange), 10% (green) and 25% (blue) additional SNPs. c) Demographic history simulated with 5% (orange), 10% (green) and 25% (blue) of additional and missing SNPs. d) Demographic history simulated with no SNP call error.

402 **3.3.2 Specific scaffold parameters**

403 We here analyze simulated sequence data where scaffolds either have or do not have
404 the same recombination and mutation rates, and are analyzed assuming scaffolds do
405 share or do not share recombination and mutation rates. We can see on Figure 6 that
406 when scaffolds all share the same parameter values, estimated demography is accurate
407 both when the analysis assumed shared or differing mutation and recombination rates.
408 However, when scaffolds are simulated with different parameter values, analyzing them
409 under the assumption that they have the same mutation and recombination rates leads
410 to poor estimations. Assuming scaffolds do not share recombination and mutation
411 rates does improve the results somewhat, but the estimations remain less accurate than
412 when scaffolds all share with same parameter values. If only the recombination rate
413 changes from one scaffold to another, the demographic history is only slightly biased,
414 whereas, if the mutation rate changes from one scaffold to the other, demographic
415 history is poorly estimated.

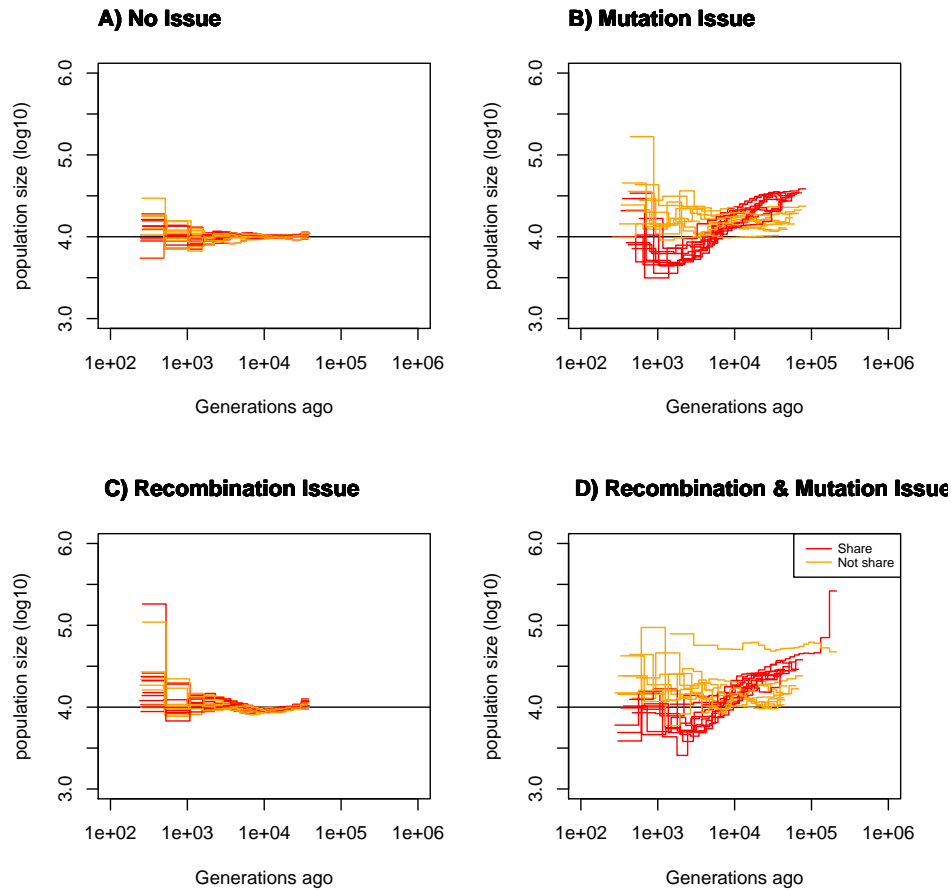


Fig. 6. Estimating demographic history using scaffolds sharing or differing in mutation and recombination rates Estimated demographic history using eSMC under a saw-tooth scenario with 10 replicates using twenty simulated scaffolds of two sequences of 2 Mb assuming scaffolds share (red) or do not share recombination and mutation rate (orange). The simulated demographic history is represented in black, for a) scaffolds share the same parameters, recombination and mutation rates are set at 1.25×10^{-8} , for b) each scaffold is randomly assigned a recombination rate between 2.5×10^{-9} and 6.25×10^{-8} and the mutation rate is 1.25×10^{-8} , for c) each scaffold is randomly assigned a mutation rate between 2.5×10^{-9} and 6.25×10^{-8} and the recombination rate is 1.25×10^{-8} and for d) each scaffold is assigned a random mutation and an independently random recombination rate, both being between 2.5×10^{-9} and 6.25×10^{-8} .

416 Even if chromosomes are fully assembled, assuming we here have one scaffold
417 of 40 Mb (chromosome fully assembled), there may be variations of the recombination
418 rate along the sequence, however this seems of little consequence when applying eSMC
419 (*i.e.* PSMC'). As can be seen in Supplementary Figure 21, the demographic scenario is
420 well inferred, despite an increase in variance and a smooth "wave" shaped demographic
421 history when sequences simulated with varying recombination rates are compared to
422 those with a fixed recombination rate throughout the genome.

423 **3.3.3 How transposable elements bias inference**

424 Transposable elements (TEs) are present in most species, and are (if detected) only
425 taken into account as missing data by SMC methods [47]). Depending on how TEs
426 affect the data set, we find that methods are more or less sensitive to them. If TEs
427 are removed from the data set, there does not appear to be any bias in the estimated
428 demographic history when using eSMC (see Figure 7), but there is an overestimation of
429 $\frac{\rho}{\theta}$ (see Table 3). We find that, the higher the proportion of sequences removed, the more
430 $\frac{\rho}{\theta}$ is over-estimated. The smaller the sequences that are removed, the more $\frac{\rho}{\theta}$ is over-
431 estimated (Tables 4 and 5). If TEs are considered to be masked in the data set (and
432 not accounted for missing data by the model), we find that this is equivalent to faulty
433 calling of SNPs, in which SNPs are missing, hence resulting in demographic history
434 estimation by eSMC similar to that observed in Figure 5a. However, if longer parts of
435 the sequences are masked by TEs, different results are obtained (see Supplementary
436 Figures 22 and 23). Indeed, there is a strong underestimation of population size and
437 the model fails to capture the correct demographic history in recent times. The longer
438 the masked parts are, the stronger the effect on the estimated demographic history.
439 Similar results are obtained with MSMC (Supplementary Figures 24, 25 and 26) and

440 MSMC2 (Supplementary Figures 27, 28 and 29).

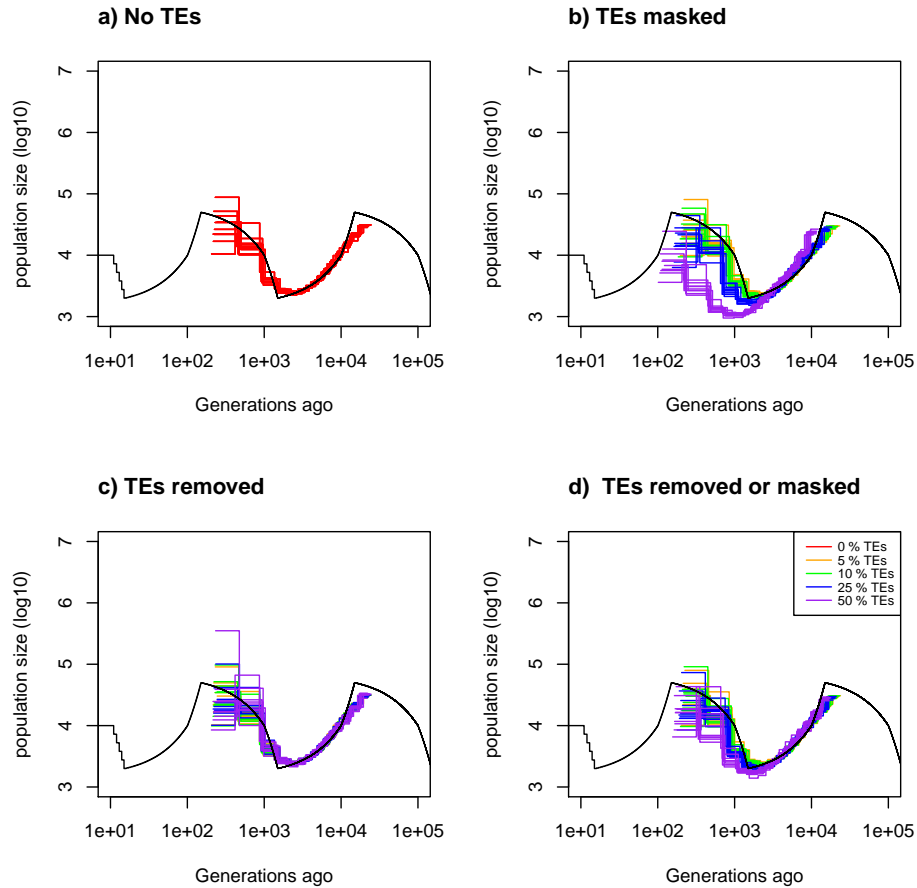


Fig. 7. Consequences of masking or removing transposable elements (TEs) from data sets. Estimated demographic history by eSMC under a saw-tooth scenario with 10 replicates using four simulated sequences of 20 Mb. The recombination and mutation rates are as in Figure 1 and the simulated demographic history is represented in black. Here the transposable elements are of length 1kbp. a) Demographic history simulated with no transposable elements. b) Demographic history simulated where transposable elements are removed. c) Demographic history simulated where TEs are masked. d) Demographic history simulated where half of transposable elements are removed and SNPs on the other half are removed. Proportion of transposable element of the genome set to 0% (red), 5% (orange), 10% (green), 25% (blue) and 50% (purple).

method	real $\frac{\rho}{\theta}$	$\frac{\rho^*}{\theta}$ and 5% TEs	$\frac{\rho^*}{\theta}$ and 10% TEs	$\frac{\rho^*}{\theta}$ and 25% TEs	$\frac{\rho^*}{\theta}$ and 50% TEs
eSMC	1	0.95 (0.021)	0.99 (0.022)	1.16 (0.10)	1.77 (0.36)
MSMC	1	1.31 (0.098)	1.35 (0.11)	1.50 (0.088)	1.91 (0.11)
MSMC2	1	0.87 (0.047)	0.88 (0.049)	1.0 (0.036)	1.35 (0.035)

Table 3: Average estimated values for the recombination over mutation ratio $\frac{\rho}{\theta}$ over ten repetitions. The coefficient of variation is indicated in brackets. TEs are removed and of length 1kb. The proportion of TEs is 5%,10% ,25% and 50%, the results are respectively displayed in column 3 to 6.

method	real $\frac{\rho}{\theta}$	$\frac{\rho^*}{\theta}$ and 5% TEs	$\frac{\rho^*}{\theta}$ and 10% TEs	$\frac{\rho^*}{\theta}$ and 25% TEs	$\frac{\rho^*}{\theta}$ and 50% TEs
eSMC	1	0.96 (0.053)	0.98 (0.066)	1.10 (0.18)	1.36 (0.41)
MSMC	1	1.38 (0.074)	1.41 (0.090)	1.54 (0.11)	1.68 (0.13)
MSMC2	1	0.87 (0.064)	0.89 (0.067)	.99 (0.15)	1.13 (0.30)

Table 4: Average estimated values for the recombination over mutation ratio $\frac{\rho}{\theta}$ over ten repetitions. The coefficient of variation is indicated in brackets. TEs are removed and of length 10kb. The proportion of TEs is 5%,10% ,25% and 50%.

method	real $\frac{\rho}{\theta}$	$\frac{\rho^*}{\theta}$ and 5% TEs	$\frac{\rho^*}{\theta}$ and 10% TEs	$\frac{\rho^*}{\theta}$ and 25% TEs	$\frac{\rho^*}{\theta}$ and 50% TEs
eSMC	1	0.95 (0.047)	0.95 (0.051)	0.98 (0.070)	1.0 (0.12)
MSMC	1	1.36 (0.048)	1.36 (0.062)	1.40 (0.093)	1.49 (0.12)
MSMC2	1	0.87 (0.056)	0.88 (0.050)	0.91 (0.079)	0.91 (0.073)

Table 5: Average estimated values for the recombination over mutation ratio $\frac{\rho}{\theta}$ over ten repetitions. The coefficient of variation is indicated in brackets. TEs are removed and of length 100kb. The proportion of TEs is 5%,10% ,25% and 50%.

441 4 Discussion

442 Throughout this work we have outlined the limits of PSMC' and MSMC methodolo-
443 gies, which had, until now, not been clearly defined. We find that, in most cases, if
444 enough genealogies (*i.e.* data) are inputted then the demographic history is perfectly
445 estimated, tending to results obtained by [13] or [8]. In [13] and [8] they use the
446 actual series of coalescence time for estimation whereas we use the series of hidden
447 states build from the discretization of time summarized in a simple matrix. However,
448 we find that the amount of data required for a perfect fit depends on the underlying
449 demographic scenario. In addition, some scenarios are better retrieved either with
450 MSMC or PSMC', indicating complementary convergence properties of MSMC and
451 PSMC' methodologies.

452 We develop a method to indicate if the amount of data is enough to retrieve
453 a specific scenario, notably by calculating the coefficient of variation of the transition
454 matrix using either real or simulated data, and therefore offer guidelines to build
455 appropriate data sets (see also Supplementary Figure 8). Our approach can also be
456 used to infer demographic history given a sequence of genealogies (using trees in Newick
457 format or sequences of coalescence events), independently of how the genealogy has
458 been estimated. Our results suggest that whole genome polymorphism data can be
459 summarized in a transition matrix based on the SMC theory to estimate demographic
460 history. As new methods can infer genealogy better and faster [55, 22, 35, 41], the
461 estimated transition matrix could become a powerful summary statistic in the future.
462 HMM can be a computational burden depending on the model and model parameters,
463 and estimating genealogy through more efficient methods would still allow the use of
464 SMC theory for parameter estimation or hypothesis testing (as in [64, 13, 19]). In

465 addition, using the work of [63], one could potentially extend our approach to account
466 for population structure.

467 We have also demonstrated that the power of PSMC', MSMC, and other SMC
468 based methods, rely on their ability to correctly infer the genealogy along the sequence
469 (*i.e.* the ancestral recombination graph). The accuracy of the ARG inference by SMC
470 methods, however, depends on the ratio of the recombination over the mutation rate
471 ($\frac{\rho}{\theta}$). As this rate increases, estimations lose accuracy. Specifically, increasing $\frac{\rho}{\theta}$ leads
472 to an over-estimation of hidden states on the diagonal, which explains the underesti-
473 mation of the recombination rate and inaccurate demographic history estimations, as
474 shown in [60, 50]. As a way around this issue, in some cases it is possible to obtain
475 better results by increasing the number of iterations. MSMC's demographic inference
476 is more sensitive to $\frac{\rho}{\theta}$ but the quality of the estimation of the ratio itself is not greatly
477 affected. This once again shows the complementarity of PSMC' and MSMC. If the
478 variable of interest is $\frac{\rho}{\theta}$, then MSMC should be used, but if the demographic his-
479 tory is of greater importance, PSMC'-based methods should be used. The amplitude
480 of population size variation also influences the estimation of hidden states along the
481 sequences, with high amplitudes leading to a poor estimation of the transition ma-
482 trix, distorting the inferred demography. We find that increasing the size of the time
483 window increases the variance of the estimations, despite using the same number of
484 parameters, as this results in a small under-estimation of $\frac{\rho}{\theta}$. In addition the complete
485 and incomplete Baum-Welch algorithms lead to identical results, demonstrating that
486 all the information required for the inference is in the estimated transition matrix.

487 Finally, we explored how imperfect data sets (due to errors in SNP calling,
488 the presence of transposable elements and existing variation in recombination and

489 mutation rates) could affect the inferences obtained using SMC based methods. We
490 show that a data set with more than 10% of spurious SNPs will lead to poor estimations
491 of the demographic history, whereas missing SNPs have a lesser effect. It is thus
492 better to be stringent during SNP calling, as false data is worse than missing data.
493 Note, however, that this consideration is valid for demographic inference under a
494 neutral model of evolution, while biases in SNP calling also affect the inference of
495 selection (especially for conserved genes under purifying selection). However, if missing
496 SNPs are structured along the sequence (as would be the case with TEs), there is a
497 strong effect on inference. It is therefore recommended that checks should be run to
498 detect regions with abnormal distributions of SNPs along the genome. Surprisingly,
499 simulation results suggest that removing random pieces of sequences have no impact
500 on the estimated demographic history. Taking this into account, when seeking to infer
501 demographic history, it seems better to remove sections of sequences than to introduce
502 sequences with SNP call errors or abnormal SNP distributions. However, removing
503 sequences leads to an over-estimation of $\frac{\rho}{\theta}$, which seems to depend on the number and
504 size of the removed sections. The removal of a few, albeit long sequences, will have
505 almost no impact, whereas removing many short sections of the sequences will lead
506 to a large overestimation of $\frac{\rho}{\theta}$. This consequence could provide an explanation for
507 the frequent overestimation of $\frac{\rho}{\theta}$ when compared to empirical measures of the ratio
508 of recombination and mutation rates $\frac{r}{\mu}$. This implies, that in some cases, despite an
509 inferred $\frac{\rho}{\theta} > 1$, the inferred demographic history can surprisingly be trusted. Note
510 also that as discussed in [50], the discrepancy between $\frac{\rho}{\theta}$ and $\frac{r}{\mu}$ can be due to life
511 history traits such as selfing or dormancy.

512 Simulation results suggest that any variation of the recombination rate along

513 the sequence does not bias demographic inference but slightly increases the variance
514 of the results and leads to small waves in the demographic history (as consequences
515 of erroneously estimated hidden state transition events because of the non constant
516 recombination rate along the sequence). Those results are similar to the one obtained
517 in [25]. On the other hand, if scaffolds do not share similar rates of mutation and
518 recombination, but are analyzed together assuming that they do, estimations will be
519 very poor. This results is surprisingly different than those obtained in [25] (although
520 the variation of mutation rate was within a scaffold in their study). This discrepancy
521 could suggest analyses based on longer scaffold to be more robust. However, this
522 problem can be avoided if each scaffold is assumed to have its own parameter values,
523 although this would increase computation time. In addition, it could provide useful
524 insight in unveiling any variation in molecular forces along the genome, albeit in a
525 coarser way than in [1].

526 4.1 Guidelines when applying SMC-based methods

527 Our aim through this work is to provide guidelines to optimize the use of SMC-based
528 methods for inference. First, if the data set is not yet built, but there is some intuition
529 concerning the demographic history and knowledge of some genomic properties of a
530 species (*e.g.* recombination and mutation rates), we recommend simulating a data
531 set corresponding to the potential scenarios. From these simulations, the transition
532 matrix for PSMC' or MSMC based methods can be built using the R package eSMC2.
533 The results obtained can guide users when it comes to the amount and quality of data
534 needed (sequence size and copy number) for a good inference. Beyond being used
535 to guide the building of data sets, it is possible to asses trustworthiness of results
536 obtained using SMC-based methods on existing data sets. If the estimated transition

537 matrix is empty in some places (*i.e.* no observed transition event between two specific
538 hidden states; white squares in Figure 1), it could suggest a lack of data and/or strong
539 variation of the population size somewhere in time. In order to test the accuracy of the
540 inferred demography, the estimated demographic history can be retrieved and used to
541 simulate a data set with more sequences and/or simulate a demographic history with
542 a higher amplitude than the estimated one. The SMC method can then be run on
543 the simulated data in order to check whether using more data results in a matching
544 scenario or if a higher amplitude of population size can indeed be inferred, in which
545 cases the initial results are most probably trustworthy.

546 As mentioned above, it is better to sequence fewer individuals, but have data
547 of better quality. It is also important to note, that more data is not necessarily always
548 better, especially if there is a risk of spurious SNPs (see Figure 5). In some cases,
549 methods are limited by their own theoretical framework, hence no given data set will
550 ever allow a correct demographic inference. In such cases, other methods based on a
551 different theoretical frameworks (*e.g.* SFS and ABC) might perform better [3, 48].

552 4.2 Concluding remarks

553 Here we present a simple method to help assess how accurate inferences obtained us-
554 ing PSMC' and MSMC would be, when applied to data sets with suspected flaws or
555 limitations. We also offer new interpretations of results obtained when hypotheses
556 are known to be violated, and thus offer an explanation as to why results sometimes
557 deviate from expectations (*e.g.* when the estimated ratio of recombination over mu-
558 tation is larger than the one measured experimentally). We propose guidelines for
559 building/evaluating data sets when using SMC-based models, as well as a method

560 which can be used to estimate the demographic history and recombination rate given
561 a genealogy (in the same spirit as Popsicle [13]). The estimated transition matrix is
562 introduced as a summary statistic, which can be used to recover demographic history
563 (more precisely the Inverse Instantaneous Coalescence Rate interpretation of popula-
564 tion size variation, when assuming panmictic population [8, 46]). This statistic could,
565 in future, be used in more complex scenarios, without the computational load of Hid-
566 den Markov models. When faced with complex demographic histories, or $\frac{\rho}{\theta} > 1$, we
567 show that there are strategies that would allow those wishing to use SMC methodology
568 to make the best use of their data.

599 5 Acknowledgments

570 This work was funded by 8097/1 *Deutsche Forschungsgemeinschaft* (<https://www.dfg.de/>)
571 to AT. DAA was funded by the Alexander von Humboldt Stiftung ([https://www.humboldt-
572 foundation.de/web/home.html](https://www.humboldt-
572 foundation.de/web/home.html)).

573 References

- 574 [1] Gustavo V. Barroso, Natasa Puzovic, and Julien Y. Dutheil. Inference of recomb-
575 nation maps from a single pair of genomes and its application to ancient samples.
576 *PLOS GENETICS*, 15(11), NOV 2019.
- 577 [2] Champak R. Beeravolu, Michael J. Hickerson, Laurent A. F. Frantz, and Konrad
578 Lohse. ABLE: blockwise site frequency spectra for inferring complex popula-
579 tion histories and recombination. *Genome Biology*, Year = 2018, Volume = 19,
580 Month = SEP 25, DOI = 10.1186/s13059-018-1517-y, Article-Number = 145,
581 ISSN = 1474-760X, ORCID-Numbers = Beeravolu Reddy, Champak/0000-0002-

582 0800-1994 Frantz, Laurent/0000-0001-8030-3885, Times-Cited = 3, Unique-ID
583 = ISI:000445752300004,.

584 [3] Annabel C. Beichman, Tanya N. Phung, and Kirk E. Lohmueller. Comparison
585 of Single Genome and Allele Frequency Data Reveals Discordant Demographic
586 Histories. *G3-GENES GENOMES GENETICS*, 7(11):3605–3620, NOV 2017.

587 [4] Anders Bergstrom, Shane A. McCarthy, Ruoyun Hui, Mohamed A. Almarri,
588 Qasim Ayub, Petr Danecek, Yuan Chen, Sabine Felkel, Pille Hallast, Jack Kamm,
589 Helene Blanche, Jean-Francois Deleuze, Howard Cann, Swapan Mallick, David
590 Reich, Manjinder S. Sandhu, Pontus Skoglund, Aylwyn Scally, Yali Xue, Richard
591 Durbin, and Chris Tyler-Smith. Insights into human genetic variation and popu-
592 lation history from 929 diverse genomes. *SCIENCE*, 367(6484, SI):1339+, MAR
593 20 2020.

594 [5] Sharon R. Browning, Brian L. Browning, Ying Zhou, Serena Tucci, and Joshua M.
595 Akey. Analysis of Human Sequence Data Reveals Two Pulses of Archaic Denisovan
596 Admixture. *CELL*, 173(1):53+, MAR 22 2018.

597 [6] Jun Cao, Korbinian Schneeberger, Stephan Ossowski, Torsten Guenther, Sebas-
598 tian Bender, Joffrey Fitz, Daniel Koenig, Christa Lanz, Oliver Stegle, Christoph
599 Lippert, Xi Wang, Felix Ott, Jonas Mueller, Carlos Alonso-Blanco, Karsten Borg-
600 wardt, Karl J. Schmid, and Detlef Weigel. Whole-genome sequencing of multiple
601 *Arabidopsis thaliana* populations. *Nature Genetics*, 43(10):956–U60, OCT 2011.

602 [7] Dan Chang and Beth Shapiro. Using ancient DNA and coalescent-based methods
603 to infer extinction. *Biology Letters*, 12(2), FEB 1 2016.

604 [8] Lounes Chikhi, Willy Rodriguez, Simona Grusea, Patricia Santos, Simon Boitard,

- 605 and Olivier Mazet. The IICR (inverse instantaneous coalescence rate) as a sum-
606 mary of genomic diversity: insights into demographic inference and model choice.
607 *Heredity*, 120(1):13–24, JAN 2018.
- 608 [9] Slew Woh Choo, Mike Rayko, Tze King Tan, Ranjeev Hari, Aleksey Komissarov,
609 Wei Yee Wee, Andrey A. Yurchenko, Sergey Kliver, Gaik Tamazian, Agostinho
610 Antunes, Richard K. Wilson, Wesley C. Warren, Klaus-Peter Koepfli, Patrick
611 Minx, Ksenia Krasheninnikova, Antoinette Kotze, Desire L. Dalton, Elaine Ver-
612 maak, Ian C. Paterson, Pavel Dobrynin, Frankie Thomas Sitam, Jeffrine J.
613 Rovie-Ryan, Warren E. Johnson, Aini Mohamed Yusoff, Shu-Jin Luo, Kayal Vizi
614 Karuppannan, Gang Fang, Deyou Zheng, Mark B. Gerstein, Leonard Lipovich,
615 Stephen J. O'Brien, and Guat Jah Wong. Pangolin genomes and the evolution
616 of mammalian scales and immunity. *GENOME RESEARCH*, 26(10):1312–1322,
617 OCT 2016.
- 618 [10] Robert Ekblom, Birte Brechlin, Jens Persson, Linnea Smeds, Malin Johansson,
619 Jessica Magnusson, Oystein Flagstad, and Hans Ellegren. Genome sequencing and
620 conservation genomics in the Scandinavian wolverine population. *Conservation*
621 *Biology*, 32(6):1301–1312, DEC 2018.
- 622 [11] Adam D. Ewing. Transposable element detection from whole genome sequence
623 data. *MOBILE DNA*, 6, DEC 29 2015.
- 624 [12] Andrea Fulgione, Maarten Koornneef, Fabrice Roux, Joachim Hermisson, and An-
625 gela M. Hancock. Madeiran *Arabidopsis thaliana* Reveals Ancient Long-Range
626 Colonization and Clarifies Demography in Eurasia. *Molecular Biology and Evo-*
627 *lution*, 35(3):564–574, MAR 2018.
- 628 [13] Lucie Gattepaille, Torsten Guenther, and Mattias Jakobsson. Inferring Past Ef-

- 629 fective Population Size from Distributions of Coalescent Times. *Molecular Biology*
630 *and Evolution*, 204(3):1191+, NOV 2016.
- 631 [14] Brandon S. Gaut, Danelle K. Seymour, Qingpo Liu, and Yongfeng Zhou. Demog-
632 raphy and its effects on genomic variation in crop domestication. *Nature Plants*,
633 4(8):512–520, AUG 2018.
- 634 [15] John Hawks. Introgression Makes Waves in Inferred Histories of Effective Popu-
635 lation Size. *HUMAN BIOLOGY*, 89(1):67–80, JAN 2017.
- 636 [16] Luke B. B. Hecht, Peter C. Thompson, and Benjamin M. Rosenthal. Com-
637 parative demography elucidates the longevity of parasitic and symbiotic rela-
638 tionships. *PROCEEDINGS OF THE ROYAL SOCIETY B-BIOLOGICAL SCI-*
639 *ENCES*, 285(1888), OCT 10 2018.
- 640 [17] Sarah Hendricks, Eric C. Anderson, Tiago Antao, Louis Bernatchez, Brenna R.
641 Forester, Brittany Garner, Brian K. Hand, Paul A. Hohenlohe, Martin Kardos,
642 Ben Koop, Arun Sethuraman, Robin S. Waples, and Gordon Luikart. Recent
643 advances in conservation and population genomics data analysis. *Evolutionary*
644 *Applications*, 11(8):1197–1211, SEP 2018.
- 645 [18] Asger Hobolth and Jens Ledet Jensen. Markovian approximation to the finite
646 loci coalescent with recombination along multiple sequences. *THEORETICAL*
647 *POPULATION BIOLOGY*, 98:48–58, DEC 2014.
- 648 [19] James E. Johndrow and Julia A. Palacios. Exact limits of inference in coalescent
649 models. *Theoretical Population Biology*, 125:75–93, FEB 2019.
- 650 [20] Marty Kardos, Anna Qvarnstrom, and Hans Ellegren. Inferring Individual In-
651 breeding and Demographic History from Segments of Identity by Descent in

- 652 Ficedula Flycatcher Genome Sequences. *GENETICS*, 205(3):1319–1334, MAR
653 2017.
- 654 [21] Jerome Kelleher, Alison M. Etheridge, and Gilean McVean. Efficient Coalescent
655 Simulation and Genealogical Analysis for Large Sample Sizes. *PLOS COMPUTATIONAL BIOLOGY*, 12(5), MAY 2016.
656
- 657 [22] Jerome Kelleher, Yan Wong, Anthony W. Wohns, Chaimaa Fadil, Patrick K.
658 Albers, and Gil McVean. Inferring whole-genome histories in large population
659 datasets (vol 51, pg 1330, 2019). *NATURE GENETICS*, 51(11):1660, NOV 2019.
- 660 [23] Robert Kofler. SimulaTE: simulating complex landscapes of transposable ele-
661 ments of populations. *BIOINFORMATICS*, 34(8):1419–1420, APR 15 2018.
- 662 [24] Sally C. Y. Lau, Nerida G. Wilson, Catarina N. S. Silva, and Jan M. Strugnell.
663 Detecting glacial refugia in the Southern Ocean. *ECOGRAPHY*.
- 664 [25] Heng Li and Richard Durbin. Inference of human population history from indi-
665 vidual whole-genome sequences. *Nature*, 475(7357):493–U84, JUL 28 2011.
- 666 [26] Shengbin Li, Bo Li, Cheng Cheng, Zijun Xiong, Qingbo Liu, Jianghua Lai, Han-
667 nah V. Carey, Qiong Zhang, Haibo Zheng, Shuguang Wei, Hongbo Zhang, Liao
668 Chang, Shiping Liu, Shanxin Zhang, Bing Yu, Xiaofan Zeng, Yong Hou, Wen-
669 hui Nie, Youmin Guo, Teng Chen, Jiuqiang Han, Jian Wang, Jun Wang, Chen
670 Chen, Jiankang Liu, Peter J. Stambrook, Ming Xu, Guojie Zhang, M. Thomas P.
671 Gilbert, Huanming Yang, Erich D. Jarvis, Jun Yu, and Jianqun Yan. Genomic
672 signatures of near-extinction and rebirth of the crested ibis and other endangered
673 bird species. *GENOME BIOLOGY*, 15(12), 2014.

- 674 [27] Michael Lynch, Ryan Gutenkunst, Matthew Ackerman, Ken Spitze, Zhiqiang
675 Ye, Takahiro Maruki, and Zhiyuan Jia. Population Genomics of *Daphnia pulex*.
676 *Molecular Biology and Evolution*, 206(1):315–332, MAY 2017.
- 677 [28] Michael Lynch, Bernhard Haubold, Peter Pfaffelhuber, and Takahiro Maruki.
678 Inference of Historical Population-Size Changes with Allele-Frequency Data. *G3-*
679 *GENES GENOMES GENETICS*, 10(1):211–223, JAN 2020.
- 680 [29] Anna-Sapfo Malaspinas, Michael C. Westaway, Craig Muller, Vitor C. Sousa,
681 Oscar Lao, Isabel Alves, Anders Bergstrom, Georgios Athanasiadis, Jade Y.
682 Cheng, Jacob E. Crawford, Tim H. Heupink, Enrico Macholdt, Stephan Peischl,
683 Simon Rasmussen, Stephan Schiffels, Sankar Subramanian, Joanne L. Wright,
684 Anders Albrechtsen, Chiara Barbieri, Isabelle Dupanloup, Anders Eriksson,
685 Ashot Margaryan, Ida Moltke, Irina Pugach, Thorfinn S. Korneliussen, Ivan P.
686 Levkivskiy, J. Vctor Moreno-Mayar, Shengyu Ni, Fernando Racimo, Martin
687 Sikora, Yali Xue, Farhang A. Aghakhanian, Nicolas Brucato, Soren Brunak,
688 Paula F. Campos, Warren Clark, Sturla Ellingvag, Gudjugudju Fourmile, Pas-
689 cale Gerbault, Darren Injie, George Koki, Matthew Leavesley, Betty Logan,
690 Aubrey Lynch, Elizabeth A. Matisoo-Smith, Peter J. McAllister, Alexander J.
691 Mentzer, Mait Metspalu, Andrea B. Migliano, Les Murgha, Maude E. Phipps,
692 William Pomat, Doc Reynolds, Francois-Xavier Ricaut, Peter Siba, Mark G.
693 Thomas, Thomas Wales, Colleen Ma’run Wall, Stephen J. Oppenheimer, Chris
694 Tyler-Smith, Richard Durbin, Joe Dortch, Andrea Manica, Mikkel H. Schierup,
695 Robert A. Foley, Marta Mirazon Lahr, Claire Bowern, Jeffrey D. Wall, Thomas
696 Mailund, Mark Stoneking, Rasmus Nielsen, Manjinder S. Sandhu, Laurent Ex-
697 coffier, David M. Lambert, and Eske Willerslev. A genomic history of Aboriginal
698 Australia. *NATURE*, 538(7624):207+, OCT 13 2016.

- 699 [30] P Marjoram and JD Wall. Fast “coalescent” simulation. *BMC Genetics*, 7, MAR
700 15 2006.
- 701 [31] Niklas Mather, Samuel M. Traves, and Simon Y. W. Ho. A practical introduction
702 to sequentially Markovian coalescent methods for estimating demographic history
703 from genomic data. *ECOLOGY AND EVOLUTION*, 10(1):579–589, JAN 2020.
- 704 [32] Maja P. Mattle-Greminger, Tugce Bilgin Sonay, Alexander Nater, Marc Pybus,
705 Tariq Desai, Guillem de Valles, Ferran Casals, Aylwyn Scally, Jaume Bertran-
706 petit, Tomas Marques-Bonet, Carel P. van Schaik, Maria Anisimova, and Michael
707 Kruetzen. Genomes reveal marked differences in the adaptive evolution between
708 orangutan species. *Genome Biology*, 19, NOV 15 2018.
- 709 [33] O. Mazet, W. Rodriguez, S. Grusea, S. Boitard, and L. Chikhi. On the importance
710 of being structured: instantaneous coalescence rates and human evolution-lessons
711 for ancestral population size inference? *Heredity*, 116(4):362–371, APR 2016.
- 712 [34] GAT McVean and NJ Cardin. Approximating the coalescent with recombina-
713 tion. *Philosophical Transactions of the Royal Society B-Biological Sciences*,
714 360(1459):1387–1393, JUL 29 2005.
- 715 [35] Sajad Mirzaei and Yufeng Wu. RENT plus : an improved method for inferring lo-
716 cal genealogical trees from haplotypes with recombination. *BIOINFORMATICS*,
717 33(7):1021–1030, APR 1 2017.
- 718 [36] Krystyna Nadachowska-Brzyska, Reto Burri, Linnea Smeds, and Hans Ellegren.
719 PSMC analysis of effective population sizes in molecular ecology and its applica-
720 tion to black-and-white *Ficedula* flycatchers. *Molecular Ecology*, 25(5):1058–1072,
721 MAR 2016.

- 722 [37] Shigeki Nakagome, Richard R. Hudson, and Anna Di Rienzo. Inferring the model
723 and onset of natural selection under varying population size from the site fre-
724 quency spectrum and haplotype structure. *PROCEEDINGS OF THE ROYAL*
725 *SOCIETY B-BIOLOGICAL SCIENCES*, 286(1896), FEB 6 2019.
- 726 [38] Michael G. Nelson, Raquel S. Linheiro, and Casey M. Bergman. McClin-
727 tock: An Integrated Pipeline for Detecting Transposable Element Insertions in
728 Whole-Genome Shotgun Sequencing Data. *G3-GENES GENOMES GENETICS*,
729 7(8):2763–2778, AUG 2017.
- 730 [39] Kevin P. Oh, Cameron L. Aldridge, Jennifer S. Forbey, Carolyn Y. Dadabay, and
731 Sara J. Oyler-McCance. Conservation Genomics in the Sagebrush Sea: Population
732 Divergence, Demographic History, and Local Adaptation in Sage-Grouse (*Centro-*
733 *cercus* spp.). *GENOME BIOLOGY AND EVOLUTION*, 11(7):2023–2034, JUL
734 2019.
- 735 [40] Julia A. Palacios, John Wakeley, and Sohini Ramachandran. Bayesian Nonpara-
736 metric Inference of Population Size Changes from Sequential Genealogies. *Genet-*
737 *ics*, 201(1):281+, SEP 2015.
- 738 [41] Pier Francesco Palamara, Jonathan Terhorst, Yun S. Song, and Alkes L. Price.
739 High-throughput inference of pairwise coalescence times identifies signals of selec-
740 tion and enriched disease heritability. *NATURE GENETICS*, 50(9):1311+, SEP
741 2018.
- 742 [42] Eleftheria Palkopoulou, Mark Lipson, Swapan Mallick, Svend Nielsen, Nadin Roh-
743 land, Sina Baleka, Emil Karpinski, Atma M. Ivancevici, Thu-Hien To, Daniel
744 Kortschak, Joy M. Raison, Zhipeng Qu, Tat-Jun Chin, Kurt W. Alt, Ste-
745 fan Claesson, Love Dalen, Ross D. E. MacPhee, Harald Meller, Alfred L. Ro-

746 car, Oliver A. Ryder, David Heiman, Sarah Young, Matthew Breen, Christina
747 Williams, Bronwen L. Aken, Magali Ruffier, Elinor Karlsson, Jeremy Johnson,
748 Federica Di Palma, Jessica Alfoldi, David L. Adelsoni, Thomas Mailund, Kasper
749 Munch, Kerstin Lindblad-Toh, Michael Hofreiter, Hendrik Poinar, and David
750 Reich. A comprehensive genomic history of extinct and living elephants. *Pro-*
751 *ceedings of the National Academy of Sciences of the United States of America*,
752 115(11):E2566–E2574, MAR 13 2018.

753 [43] Eleftheria Palkopoulou, Swapan Mallick, Pontus Skoglund, Jacob Enk, Nadin
754 Rohland, Heng Li, Ayca Omrak, Sergey Vartanyan, Hendrik Poinar, Anders
755 Gotherstrom, David Reich, and Love Dalen. Complete Genomes Reveal Sig-
756 natures of Demographic and Genetic Declines in the Woolly Mammoth. *Current*
757 *Biology*, 25(10):1395–1400, MAY 18 2015.

758 [44] Austin H. Patton, Mark J. Margres, Amanda R. Stahlke, Sarah Hendricks, Kevin
759 Lewallen, Rodrigo K. Hamede, Manuel Ruiz-Aravena, Oliver Ryder, Hamish Mc-
760 Callum, I, Menna E. Jones, Paul A. Hohenlohe, and Andrew Storfer. Contem-
761 porary Demographic Reconstruction Methods Are Robust to Genome Assembly
762 Quality: A Case Study in Tasmanian Devils. *MOLECULAR BIOLOGY AND*
763 *EVOLUTION*, 36(12):2906–2921, DEC 2019.

764 [45] Javier Prado-Martinez, Peter H. Sudmant, Jeffrey M. Kidd, Heng Li, Joanna L.
765 Kelley, Belen Lorente-Galdos, Krishna R. Veeramah, August E. Woerner, Timo-
766 thy D. O’Connor, Gabriel Santpere, Alexander Cagan, Christoph Theunert, Fer-
767 ran Casals, Hafid Laayouni, Kasper Munch, Asger Hobolth, Anders E. Halager,
768 Maika Malig, Jessica Hernandez-Rodriguez, Irene Hernando-Herraez, Kay Prue-
769 fer, Marc Pybus, Laurel Johnstone, Michael Lachmann, Can Alkan, Dorina Twigg,

770 Natalia Petit, Carl Baker, Fereydoun Hormozdiari, Marcos Fernandez-Callejo,
771 Marc Dabad, Michael L. Wilson, Laurie Stevison, Cristina Camprubi, Tiago Car-
772 valho, Aurora Ruiz-Herrera, Laura Vives, Marta Mele, Teresa Abello, Ivanela
773 Kondova, Ronald E. Bontrop, Anne Pusey, Felix Lankester, John A. Kiyang,
774 Richard A. Bergl, Elizabeth Lonsdorf, Simon Myers, Mario Ventura, Pascal Gag-
775 neux, David Comas, Hans Siegismund, Julie Blanc, Lidia Agueda-Calpena, Marta
776 Gut, Lucinda Fulton, Sarah A. Tishkoff, James C. Mullikin, Richard K. Wil-
777 son, Ivo G. Gut, Mary Katherine Gonder, Oliver A. Ryder, Beatrice H. Hahn,
778 Arcadi Navarro, Joshua M. Akey, Jaume Bertranpetit, David Reich, Thomas
779 Mailund, Mikkel H. Schierup, Christina Hvilsom, Aida M. Andres, Jeffrey D.
780 Wall, Carlos D. Bustamante, Michael F. Hammer, Evan E. Eichler, and Tomas
781 Marques-Bonet. Great ape genetic diversity and population history. *NATURE*,
782 499(7459):471–475, JUL 25 2013.

783 [46] Willy Rodriguez, Olivier Mazet, Simona Grusea, Armando Arredondo, Josue M.
784 Corujo, Simon Boitard, and Lounes Chikhi. The IICR and the non-stationary
785 structured coalescent: towards demographic inference with arbitrary changes in
786 population structure. *Heredity*, 121(6):663–678, DEC 2018.

787 [47] Stephan Schiffels and Richard Durbin. Inferring human population size and sep-
788 aration history from multiple genome sequences. *Nature Genetics*, 46(8):919–925,
789 AUG 2014.

790 [48] Joshua G. Schraiber and Joshua M. Akey. Methods and models for unravelling
791 human evolutionary history. *NATURE REVIEWS GENETICS*, 16(12):727–740,
792 DEC 2015.

793 [49] Daniel R. Schrider, Alexander G. Shanku, and Andrew D. Kern. Effects of Linked

- 794 Selective Sweeps on Demographic Inference and Model Selection. *GENETICS*,
795 204(3):1207+, NOV 2016.
- 796 [50] Thibaut Paul Patrick Sellinger, Diala Abu Awad, Markus Moest, and Aurelien
797 Tellier. Inference of past demography, dormancy and self-fertilization rates from
798 whole genome sequence data. *PLOS GENETICS*, 16(4), APR 2020.
- 799 [51] Sara Sheehan, Kelley Harris, and Yun S. Song. Estimating Variable Effective
800 Population Sizes from Multiple Genomes: A Sequentially Markov Conditional
801 Sampling Distribution Approach. *Molecular Biology and Evolution*, 194(3):647+,
802 JUL 2013.
- 803 [52] Sara Sheehan and Yun S. Song. Deep Learning for Population Genetic Inference.
804 *PLOS Computational Biology*, 12(3), MAR 2016.
- 805 [53] Montgomery Slatkin. Statistical methods for analyzing ancient DNA from ho-
806 minins. *CURRENT OPINION IN GENETICS & DEVELOPMENT*, 41:72–76,
807 DEC 2016.
- 808 [54] Chris C. R. Smith and Samuel M. Flaxman. Leveraging whole genome sequenc-
809 ing data for demographic inference with approximate Bayesian computation.
810 *MOLECULAR ECOLOGY RESOURCES*, 20(1):125–139, JAN 2020.
- 811 [55] Leo Speidel, Marie Forest, Sinan Shi, and Simon R. Myers. A method for genome-
812 wide genealogy estimation for thousands of samples. *NATURE GENETICS*,
813 51(9):1321+, SEP 2019.
- 814 [56] Jeffrey P. Spence, Matthias Steinrucken, Jonathan Terhorst, and Yun S. Song.
815 Inference of population history using coalescent HMMs: review and outlook. *Cur-
816 rent Opinion in Genetics & Development*, 53:70–76, DEC 2018.

- 817 [57] Paul R. Staab, Sha Zhu, Dirk Metzler, and Gerton Lunter. *scrm*: efficiently
818 simulating long sequences using the approximated coalescent with recombination.
819 *Bioinformatics*, 31(10):1680–1682, MAY 15 2015.
- 820 [58] Remco Stam, Tetyana Nosenko, Anja C. Hoerger, Wolfgang Stephan, Michael
821 Seidel, Jose M. M. Kuhn, Georg Haberer, and Aurelien Tellier. The de Novo
822 Reference Genome and Transcriptome Assemblies of the Wild Tomato Species
823 *Solanum chilense* Highlights Birth and Death of NLR Genes Between Tomato
824 Species. *G3-GENES GENOMES GENETICS*, 9(12):3933–3941, DEC 2019.
- 825 [59] Matthias Steinrucken, Jack Kamm, Jeffrey P. Spence, and Yun S. Song. Inference
826 of complex population histories using whole-genome sequences from multiple pop-
827 ulations. *PROCEEDINGS OF THE NATIONAL ACADEMY OF SCIENCES*
828 *OF THE UNITED STATES OF AMERICA*, 116(34):17115–17120, AUG 20 2019.
- 829 [60] Jonathan Terhorst, John A. Kamm, and Yun S. Song. Robust and scalable in-
830 ference of population history froth hundreds of unphased whole genomes. *Nature*
831 *Genetics*, 49(2):303–309, FEB 2017.
- 832 [61] Jonathan Terhorst and Yun S. Song. Fundamental limits on the accuracy of
833 demographic inference based on the sample frequency spectrum. *Proceedings of*
834 *the National Academy of Sciences of the United States of America*, 112(25):7677–
835 7682, JUN 23 2015.
- 836 [62] Berit Lindum Waltoft and Asger Hobolth. Non-parametric estimation of popu-
837 lation size changes from the site frequency spectrum. *Statistical Applications in*
838 *Genetics and Molecular Biology*, 17(3), JUN 2018.
- 839 [63] Ke Wang, Iain Mathieson, Jared O’Connell, and Stephan Schiffels. Tracking

- 840 human population structure through time from whole genome sequences. *PLOS*
841 *GENETICS*, 16(3), MAR 2020.
- 842 [64] Pengcheng Wang, Hongyan Yao, Kadeem J. Gilbert, Qi Lu, Yu Hao, Zhengwang
843 Zhang, and Nan Wang. Glaciation-based isolation contributed to speciation in a
844 Palearctic alpine biodiversity hotspot: Evidence from endemic species. *Molecular*
845 *Phylogenetics and Evolution*, 129:315–324, DEC 2018.
- 846 [65] Rachel C. Williams, Marina B. Blanco, Jelmer W. Poelstra, Kelsie E. Hunnicutt,
847 Aaron A. Comeault, and Anne D. Yoder. Conservation genomic analysis reveals
848 ancient introgression and declining levels of genetic diversity in Madagascar’s
849 hibernating dwarf lemurs. *HEREDITY*, 124(1):236–251, JAN 2020.
- 850 [66] C Wiuf and J Hein. Recombination as a point process along sequences. *Theoretical*
851 *Population Biology*, 55(3):248–259, JUN 1999.
- 852 [67] Chee-Wei Yew, Dongsheng Lu, Lian Deng, Lai-Ping Wong, Rick Twee-Hee Ong,
853 Yan Lu, Xiaoji Wang, Yushimah Yunus, Farhang Aghakhanian, Siti Shuhada
854 Mokhtar, Mohammad Zahirul Hoque, Christopher Lok-Yung Voo, Thuhairah Ab-
855 dul Rahman, Jong Bhak, Maude E. Phipps, Shuhua Xu, Yik-Ying Teo, Sub-
856 biah Vijay Kumar, and Boon-Peng Hoh. Genomic structure of the native in-
857 habitants of Peninsular Malaysia and North Borneo suggests complex human
858 population history in Southeast Asia. *Human Genetics*, 137(2):161–173, FEB
859 2018.